J Physiol 587.21 (2009) pp 5275–5288

The Journal of Physiology

Nerve-evoked purinergic signalling suppresses action potentials, Ca^{2+} flashes and contractility evoked by muscarinic receptor activation in mouse urinary bladder smooth muscle

Thomas J. Heppner[1], Matthias E. Werner[2], Bernhard Nausch[1], Catherine Vial[3], Richard J. Evans[3] and Mark T. Nelson[1,2]

[1]*Department of Pharmacology, University of Vermont, Burlington, VT 05405, USA*
[2]*Division of Cardiovascular and Endocrine Sciences, University of Manchester, Manchester M13 9NT, UK*
[3]*Department of Cell Physiology & Pharmacology, University of Leicester, Leicester LEI 9HN, UK*

Contraction of urinary bladder smooth muscle (UBSM) is caused by the release of ATP and ACh from parasympathetic nerves. Although both purinergic and muscarinic pathways are important to contraction, their relative contributions and signalling mechanisms are not well understood. Here, the contributions of each pathway to urinary bladder contraction and the underlying electrical and Ca^{2+} signalling events were examined in UBSM strips from wild type mice and mice deficient in P2X1 receptors ($P2X1^{-/-}$) before and after pharmacological inhibition of purinergic and muscarinic receptors. Electrical field stimulation was used to excite parasympathetic nerves to increase action potentials, Ca^{2+} flash frequency, and force. Loss of P2X1 function not only eliminated action potentials and Ca^{2+} flashes during stimulation, but it also led to a significant increase in Ca^{2+} flashes following stimulation and a corresponding increase in the force transient. Block of muscarinic receptors did not affect action potentials or Ca^{2+} flashes during stimulation, but prevented them following stimulation. These findings indicate that nerve excitation leads to rapid engagement of smooth muscle P2X1 receptors to increase action potentials (Ca^{2+} flashes) during stimulation, and a delayed increase in excitability in response to muscarinic receptor activation. Together, purinergic and muscarinic stimulation shape the time course of force transients. Furthermore, this study reveals a novel inhibitory effect of P2X1 receptor activation on subsequent increases in muscarinic-driven excitability and force generation.

(Resubmitted 18 July 2009; accepted after revision 26 August 2009; first published online 7 September 2009)
Corresponding author T. J. Heppner: Department of Pharmacology, Given Bldg, Room C315, 89 Beaumont Avenue, University of Vermont, Burlington, VT 05405-0068, USA. Email: thomas.heppner@uvm.edu

Abbreviations α,β-meATP, α,β-methyleneATP; AUC, area under the curve; BK, large conductance calcium-activated K^+ channel; CPA, cyclopiazonic acid; DHIC, detrusor hyperactivity with impaired contractile function; EFS, electrical field stimulation; K_v, voltage-dependent K^+ channel; PSS, physiological salt solution; P2X1R, P2X1 receptor; SK, small conductance calcium-activated K^+ channel; UB, urinary bladder; UBSM, urinary bladder smooth muscle; WT, wild type.

Introduction

Voiding of urine from the urinary bladder is caused by the activation of parasympathetic nerves and the co-release of the neurotransmitters ATP and ACh to cause contraction of the urinary bladder smooth muscle (UBSM) (Burnstock, 2009). ATP activates P2X1 receptor (P2X1R) channels in the UBSM membrane to cause the depolarizing influx of Ca^{2+} and Na^+, measured as local purinergic Ca^{2+} transients (Heppner *et al.* 2005) that cause an excitatory junction potential (Hashitani *et al.* 2000; Young *et al.* 2008). The slower, metabotropic cholinergic response is mediated by activation of G-protein-coupled muscarinic receptor subtypes M_2 and M_3 (Andersson & Arner, 2004). M_3 receptors are thought to play the dominant role in generating contractile force (Matsui *et al.* 2000; Yamanishi *et al.* 2000; Fetscher *et al.* 2002). M_3 receptors are coupled to $G_{q/11}$, which activates

DOI: 10.1113/jphysiol.2009.178806

phosphoinositide hydrolysis and Ca^{2+} mobilization through InsP_3 receptors located on the sarcoplasmic reticulum (Iacovou *et al.* 1990). In addition, Ca^{2+} entry through L-type voltage-dependent Ca^{2+} channels and the Rho–kinase pathway appear to be involved in contraction (Abrams & Andersson, 2007).

The relative contributions of purinergic and muscarinic pathways to UB contraction appear to vary depending on species and disease states (Andersson, 2003). For example, purinergic signalling becomes more prominent in human UB with interstitial cystitis or partial outlet obstruction (Palea *et al.* 1993; Bayliss *et al.* 1999; O'Reilly *et al.* 2001). However, in many cases, the contributions of the two pathways have been assessed by measuring the effects of receptor inhibitors on peak force generation, assuming independence of pathway action. The purinergic pathway plays a greater role at lower stimulation frequencies (Werner *et al.* 2007). Given the different temporal aspects of purinergic and muscarinic actions and overlapping mechanisms, this may be an inappropriate assumption.

The translation of excitatory nerve impulses through purinergic and muscarinic pathways to urinary bladder contraction is not well understood. It is, however, clear that purinergic and muscarinic signalling pathways increase Ca^{2+} levels and cell excitability through different mechanisms. The binding of ACh and ATP to their receptors induces a variety of unique Ca^{2+} signals in the detrusor smooth muscle. ATP release from nerve varicosities activates nearby P2X1 receptors to cause local Ca^{2+} transients in UBSM (Heppner *et al.* 2005) which are similar to junctional Ca^{2+} transients in mesenteric arteries (Lamont & Wier, 2002; Lamont *et al.* 2003) and neuroeffector Ca^{2+} transients in vas deferens (Brain *et al.* 2002, 2003). Muscarinic receptor activation leads to InsP_3-mediated Ca^{2+} waves (Iino, 1990; Iino *et al.* 1993; Ji *et al.* 2004; McCarron *et al.* 2004). Increases in excitability can be monitored as Ca^{2+} flashes, which reflect Ca^{2+} entry through L-type voltage-dependent Ca^{2+} channels during an action potential (Klockner & Isenberg, 1985; Heppner *et al.* 2005; Balemba *et al.* 2006).

In this study we examined the contribution of purinergic and muscarinic signalling to urinary bladder contraction as well as the underlying Ca^{2+} events that initiate force generation. We measured force, membrane potential and examined Ca^{2+} events (Ca^{2+} flashes and Ca^{2+} waves) evoked by nerve stimulation with purinergic and muscarinic receptor inhibition in normal and in mice that are deficient in the P2X1 receptor subtype ($P2X1^{-/-}$). P2X1 receptors mediate purinergic signalling in urinary bladder smooth muscle (Vial & Evans, 2000). We found that the purinergic-driven increases in UBSM excitability precede the muscarinic effects, and that inhibition or loss of P2X1Rs leads to an increase in muscarinic excitability and force generation. We have identified a novel postsynaptic interaction of purinergic and muscarinic signalling to modulate nerve-evoked force and Ca^{2+} events in urinary bladder smooth muscle, such that purinergic activation acts to decrease the response to muscarinic stimulation.

Methods

Ethical approval

All animal procedures comply with the policies and regulations pertaining to animal research (Drummond, 2009) and were conducted according to the Guide for the Care and Use of Laboratory Animals (USA) and approved by the Office of Animal Care Management at the University of Vermont. Adult male mice (C57Bl6) and P2X1-deficient ($P2X1^{-/-}$) mice were killed by pentobarbital sodium followed by thoracotomy or decapitation. A total of 56 mice including 11 $P2X1^{-/-}$ mice were used in this study. The urinary bladder was quickly removed and placed in cold Hepes-buffered solution. For Ca^{2+} imaging or electrophysiology, thin UBSM strips were removed from the serosal surface, and for myography the UBSM layer was dissected free of the urothelium and suburothelium. All experiments were conducted at 35–37°C in a bicarbonate-buffered physiological salt solution (PSS), continuously bubbled with 95% oxygen and 5% carbon dioxide.

Myography

Force measurements were performed and analysed as in prior publications (Herrera *et al.* 2005; Werner *et al.* 2007). Briefly, force production of strips (8 strips per bladder; 2–3 mm wide and 5–7 mm long) in response to electrical field stimulation (EFS) was measured using a MyoMed myograph (MED Associates, Georgia, VT, USA). Frequency–response curves were created by measuring the EFS-induced contraction amplitude at stimulus frequencies of 0.5, 2, 3.5, 5, 7.5, 10, 12.5, 15, 20, 30, 40 and 50 Hz. To investigate EFS-induced force kinetics, the rate of rise (peak force divided by the time from beginning of the contraction to the peak amplitude), the rate of decay (peak force divided by the time from the peak amplitude to the return to baseline), duration of force transient (half-width, duration of the force transient at 50% of the maximum amplitude) were measured, and the area under the curve (AUC) determined as the integral of the force transient 10% above baseline.

Pulse amplitude was 20 V, and polarity was reversed for alternating pulses. Pulse width was 0.2 ms, and stimulus duration was 2 s. Stimuli were applied every 3 min using a model PHM-152V stimulator (MED Associates). After the first frequency–response curve was generated, the UBSM strips were washed 3 times. Fifteen minutes after

the final wash pharmacological compounds were added directly to the tissue bath. Strips were incubated in the presence of the compounds for 15 min, and then a second frequency–response curve was generated using the same EFS parameters.

Ca^{2+} imaging and analysis

Thin strips of detrusor were pinned to small Sylgard blocks and placed in a chamber specially designed to maintain constant flow and to measure rapid Ca^{2+} responses. To allow fresh, oxygenated PSS to reach the tissue, thin spacers (0.2 mm) were placed on either side of the tissue strip to elevate the tissue and Sylgard block off the chamber bottom. The tissue was superfused (1–2 ml min^{-1}). Drugs were dissolved in the superfusing PSS and applied for at least 10 min prior to image acquisition unless otherwise indicated.

Ca^{2+} events were imaged with a laser scanning confocal microscope (Oz; Noran Instruments) attached to a Nikon diaphot microscope. A Nikon ×60 water immersion objective (NA 1.2) was used to visualize the tissue. Images were acquired using a software package (Prairie Technologies, Inc., Middleton, WI, USA) controlled by an OZ-PC workstation. To visualize Ca^{2+} events in UBSM, the tissue was placed in a Hepes solution containing the Ca^{2+}-sensitive fluorescent dye, fluo-4 AM (10 μM) (Invitrogen, Eugene, OR, USA) and Pluronic F-127 (2.5 μg ml^{-1}; Invitrogen, Eugene, OR, USA). To facilitate loading of the dye, the tissue was kept in the dark for 60–90 min at 21–23°C followed by a wash in normal Hepes-buffered solution (21–23°C) before placing the tissue in PSS. A krypton–argon laser was used to excite fluo-4 (488 nm) and the emitted light was captured at wavelengths >500 nm. The acquisition rate for most experiments was 53 images s^{-1} (one image every 18.9 ms). The size of the field was 131 μm × 131 μm (250 pixels × 250 pixels). The nerves in the strip were excited with platinum electrodes placed in the recording chamber which were attached to the output of the stimulus isolation unit of a Grass S44 stimulator. Voltages used to evoke Ca^{2+} transients ranged from 100 to 140 V. A train of stimuli was applied for 1 s at a frequency of 10–30 Hz, using a 0.2 ms pulse duration. Individual Ca^{2+} flashes could be most easily detected at a frequency of 10 Hz, and this frequency was used to quantify events during a stimulus train. Image analysis was conducted offline using customized software written in our laboratory (Dr. Adrian Bonev).

Each experiment consisted of a 25–30 s recording from the same field during which a 1 s stimulus train (10–30 Hz) was applied. The same field was used before and after drug treatment to allow us to measure Ca^{2+} events in the same UBSM bundle. One to three files were recorded under control conditions and after drug application. The time interval between each file was at least 5 min.

Electrophysiology

Thin strips of detrusor containing a single layer of smooth muscle were pinned to the Sylgard bottom of a recording chamber and superfused (3 ml min^{-1}) with oxygenated PSS. Individual smooth muscle cells were impaled with sharp electrodes filled with 0.5 M KCl having a resistance of 200 ± 25 MΩ. The acquisition rate was 2 kHz and the signal was amplified with an Axoclamp 2A amplifier (Axon Instruments/Molecular Devices, CA, USA). Data were recorded and analysed using pClamp software (Axon Instruments/Molecular Devices). To evoke action potentials, the parasympathetic nerve fibres were stimulated by EFS via platinum electrodes on either side of the tissue. Stimuli were generated by a Grass S44 stimulator and delivered for 1 s at a frequency of 20 Hz. The duration of a single pulse was 0.2 ms (18–145 V). Inhibitors of purinergic or muscarinic receptors were added to the superfusing PSS and the tissue was allowed to incubate for at least 10 min.

Solutions and drugs

UBSM strips were removed from the urinary bladder in Hepes solution with the following composition (mM): NaCl, 134; KCl, 6; $MgCl_2$, 1; $CaCl_2$, 2; Hepes, 10; glucose, 10; (pH 7.4). NaOH was used to adjust the pH of Hepes solutions. PSS had the following composition (in mM): NaCl, 119; KCl, 4.7; $NaHCO_3$, 23.8; KH_2PO_4, 1.2; $CaCl_2$, 1.6; $MgCl_2$, 1.2, EDTA, 0.023; and glucose, 11.0 (pH 7.4). PSS was continuously bubbled with 95% O_2–5% CO_2. Atropine, α,β-methylene ATP (α,β-meATP) and suramin were obtained from Sigma-Aldrich (St Louis, MO, USA).

Statistics

Data are expressed as mean ± S.E.M. (n) refers to the number of events or the number of preparations as indicated in the text. To determine significance, the appropriate Student's t test (paired or unpaired) was performed on the raw data. Significance was determined at $P \leq 0.05$.

Results

Contributions of purinergic and muscarinic signalling to urinary bladder contractions

Urinary bladder smooth muscle (UBSM) contraction is caused by the co-release of ATP and ACh from parasympathetic nerve varicosities. ATP and ACh activate

two distinct excitatory pathways: the purinergic pathway mediated through purinergic (P2X1) receptor channels and the cholinergic pathway mediated through muscarinic receptors. Contributions of purinergic and muscarinic signalling to urinary bladder contractile responses have often been estimated by the reduction in nerve-evoked peak force to purinergic and muscarinic receptor inhibitors. To study the contribution of each pathway to the generation of force, contractions were recorded from mouse bladder strips using electrical field stimulation (EFS) with stimulating frequencies from 0.5–50 Hz. Force measurements under control conditions showed a frequency-dependent increase in amplitude illustrated in Fig. 1*Aa* and *b*). It has been previously demonstrated that inhibition of muscarinic and purinergic receptors by atropine and α,β-meATP, respectively, completely inhibits nerve-evoked contractions of UB strips from mouse (Takeuchi *et al.* 2008). To study the contribution of muscarinic activation to force, muscarinic receptors were inhibited by atropine (Fig. 1*Aa–Ca*). Atropine reduced peak force by 50–60% at stimulating frequencies $\geq$ 20 Hz (Fig. 1*Aa* and *Ba*). However, peak force does not provide a full view of force generation during the entire evoked transient. To measure total force, the force integral or area under the curve (AUC) was determined. The AUC indicated that the muscarinic component contributed ~50–70% of total force at frequencies $\geq$ 20 Hz (Fig. 1*Ca*). In the absence of P2X1 receptors, atropine nearly abolished

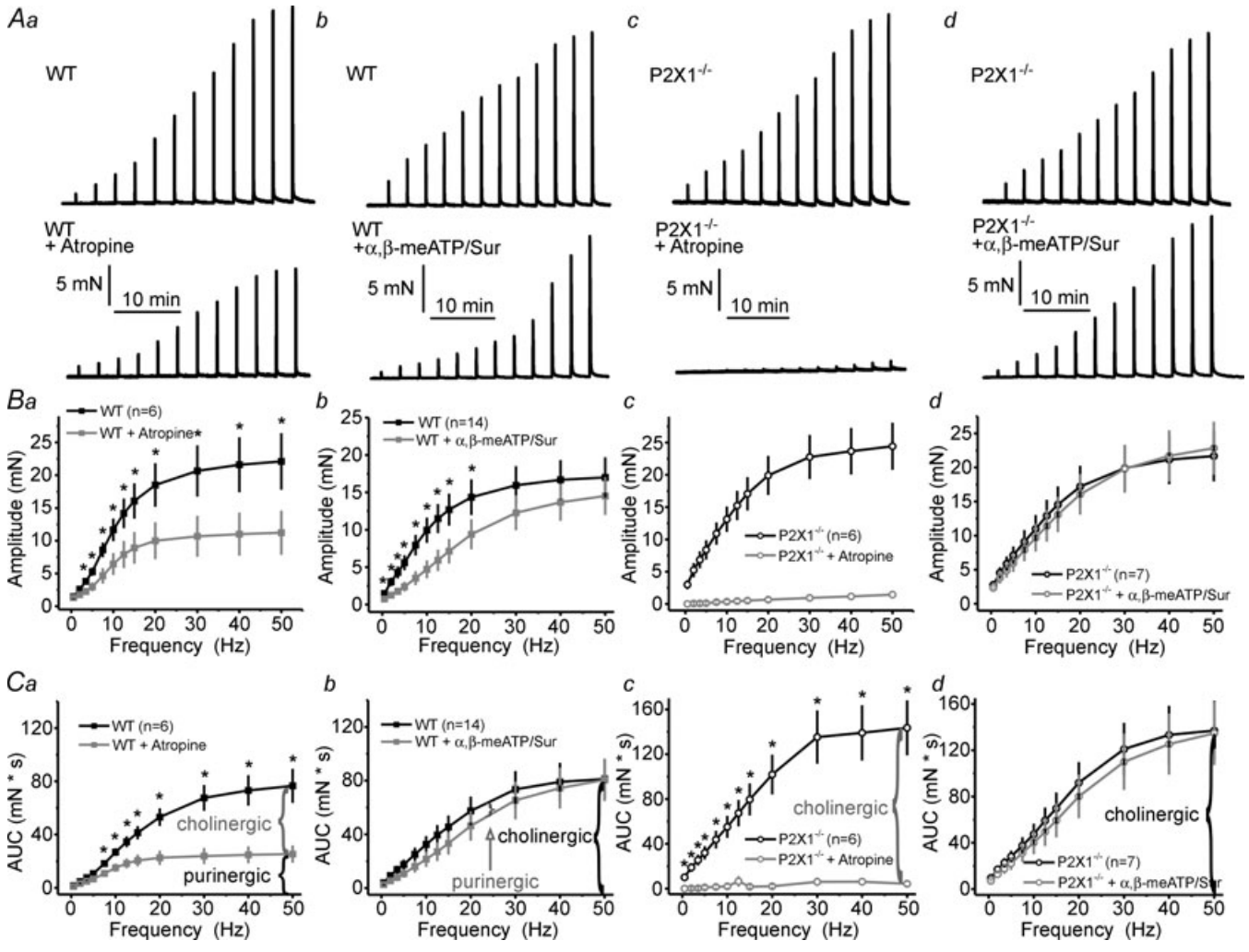

Figure 1. Differential effects of P2X1 and muscarinic receptor inhibition on EFS-induced force from wild type (WT) and P2X1$^{-/-}$ UBSM strips

Aa–Ad are representative traces showing the response to EFS (0.5–50 Hz) under control conditions and following the block of muscarinic transmission with atropine and purinergic transmission with α,β-meATP–suramin (10 μM each). The amplitude in response to different frequencies of EFS and receptor blocking (mean $\pm$ S.E.M.) are shown in *Ba–Bd*. The area under the curve (AUC) is shown in *Ca–Cd*. The contribution of each pathway to total force is labelled in black and the putative contribution of the blocked pathway is shown in grey (*Ca–Cd*). $^*P < 0.05$. *n*, number of strips from 3–6 animals.

nerve-evoked force in UBSM strips from P2X1$^{-/-}$ mice (Fig. 1*Ac–Cc*) demonstrating that contraction is dependent on purinergic and muscarinic signalling.

Based on the above results with muscarinic receptor block, it was expected that inhibition of purinergic receptors with α,β-meATP and suramin would reduce AUC and peak amplitude by 30–50% at higher frequencies. However, inhibition of purinergic receptors only reduced peak force amplitudes at lower frequencies (≤ 20 Hz) (Fig. 1*Ab* and *Bb*). Even more striking was the lack of effect of purinergic receptor inhibition on the AUC at all frequencies (Fig. 1*Cb*). Since the stimulus strength was unchanged, this indicates that the force generated by the muscarinic pathway increased significantly in response to purinergic receptor inhibition. One possible explanation for the increased muscarinic component is that purinergic signals inhibit muscarinic responses. α,β-meATP and suramin had no effect on nerve-evoked force of UBSM strips from P2X1R$^{-/-}$ mice (Fig. 1*Ad–Cd*), indicating that the actions of these drugs requires functional P2X1Rs (Vial & Evans, 2000).

P2X1$^{-/-}$ mice lack purinergic signalling and must rely entirely on muscarinic signalling for bladder contraction. A significant difference in contraction amplitude (10 Hz) between WT and P2X1$^{-/-}$ mice was found when normalized to carbachol contractions (Vial & Evans, 2000). We also found a significant difference in force (10 Hz) when the data were normalized to 60 mM K^+ contractions (0.88 ± 0.05, $n = 34$ strips WT; 0.63 ± 0.04, $n = 38$ strips P2X1$^{-/-}$; $P < 0.05$).

Inhibition of muscarinic receptors caused similar reductions in peak force and AUC (Fig. 1*Ba* and *Ca*). However, purinergic inhibition caused a significant reduction in peak force, but did not affect AUC (Fig. 1*Bb* and *Cb*) suggesting a significant increase in the duration of the force transient. This possibility was studied by measuring contraction kinetics (rate of rise and rate of decay as well as durations of force transient) in the absence of functional purinergic receptors using UBSM strips from WT and P2X1$^{-/-}$ mice (Fig. 2). The rate of increase in force to EFS is relatively fast compared to the rate of decay. Purinergic inhibition with α,β-meATP–suramin significantly slowed the rate of rise at all frequencies (Fig. 2*A* and *Aa*). This is consistent with the idea that purinergic signalling is rapid and contributes significantly to the initial rise in force (Gitterman & Evans, 2001; Lamont *et al.* 2003). The rate of decay was significantly decreased and the half-width of the force transients was significantly elevated at lower frequencies in WT (Fig. 2*A*, *Ab* and *Ac*). However, in P2X1$^{-/-}$ mice the rate of rise was similar to WT (Fig. 2*B* and *Ba*) and may reflect compensatory mechanisms during development. The rate of decay was decreased at lower frequencies and the duration of force transients was significantly elevated at all frequencies in UBSM strips from P2X1$^{-/-}$ mice, compared to WT (Fig. 2*B*, *Bb* and *Bc*). These results are consistent with the idea that P2X1 receptor activation leads to a rapid increase in excitability and Ca^{2+} entry, and suppresses subsequent muscarinic effects.

Temporal contributions of purinergic- and muscarinic-driven excitability

In guinea pig, it has been previously shown that nerve excitation causes a purinergic-driven increase in action potentials during excitation and subsequent elevation of action potentials caused by muscarinic mechanisms (Hashitani *et al.* 2000). Here, we examined this relationship in UBSM strips from mice. The membrane potential and action potentials were recorded from mouse smooth muscle cells in urinary bladder strips, using sharp microelectrodes. The resting membrane potential was -43.1 ± 1.3 mV ($n = 14$ preparations) in PSS. Action potentials occurred spontaneously or could be evoked with EFS. Using a 20 Hz (1 s duration) stimulus train, action potentials were evoked within several hundred milliseconds of the beginning of stimulation and would often continue after stimulation was stopped (Fig. 3).

To study the contribution of purinergic signalling to evoked action potentials, muscarinic receptors were blocked by atropine (10 μM). In paired experiments, muscarinic receptor block did not significantly change the membrane potential measured $\sim$10 min after the addition of atropine. Membrane potential in control was -37.3 ± 1.7 mV, and with muscarinic block -35.5 ± 1.5 mV ($n = 5$ preparations). Atropine had no effect on action potential frequency during stimulation, but it completely blocked evoked action potentials after stimulation (Fig. 3*A* and *C*). The contribution of muscarinic signalling to evoked action potentials was studied by inactivating purinergic receptors by the addition of α,β-meATP. In paired experiments, purinergic block did not significantly change the membrane potential measured $\sim$10 min after the addition of $\alpha,\beta-$meATP. Membrane potential in control was -45.3 ± 2.9 mV, and with purinergic block -45.6 ± 2.9 mV ($n = 6$ preparations). In contrast to inhibition of muscarinic receptors, inactivation of purinergic receptors prevented action potential generation during stimulation, but did not affect the elevation in action potential number following stimulation (Fig. 3*B* and *C*). Inhibition of purinergic receptors increased the time to first EFS-induced action potentials (Fig. 3*D*). Thus, purinergic signalling underlies the rapid onset of action potentials during EFS whereas muscarinic signalling increases action potential generation following EFS.

Ca^{2+} flashes and Ca^{2+} waves in UBSM

A drawback of membrane potential recordings is that action potentials are recorded from one smooth muscle

cell with each microelectrode impalement. This limits the ability to record action potentials from a large number of cells. Ca^{2+} imaging of UBSM strips permits the recording of a relatively large number of smooth muscle cells. Action potentials are measured as rapid Ca^{2+} flashes, which reflect Ca^{2+} influx through L-type voltage-dependent Ca^{2+} channels during an action potential (Klockner & Isenberg, 1985; Heppner *et al.* 2005; Balemba *et al.* 2006). In addition to Ca^{2+} flashes, Ca^{2+} waves were also detected in smooth muscle cells in UB strips. In contrast to Ca^{2+} flashes, which are very rapid and cause a nearly simultaneous increase in Ca^{2+} throughout the muscle cell, Ca^{2+} waves are much slower events that are characterized by a slower rise time and an increase in Ca^{2+} that travels as a visible wave through the smooth muscle cell (range of 42.9 to 177.5 μm s^{-1} with a mean value of 92.9 ± 12.8 μm s^{-1}; $n = 12$ Ca^{2+} waves from 4 preparations). Ca^{2+} flashes were easily distinguished from Ca^{2+} waves by their >4-fold faster rise time. The 10–90% rise time for Ca^{2+} flashes was 52.9 ± 1.9 ms ($n = 36$ flashes from 4 preparations) compared with 253.8 ± 33.7 ms for Ca^{2+} waves ($n = 20$ waves from 4 preparations).

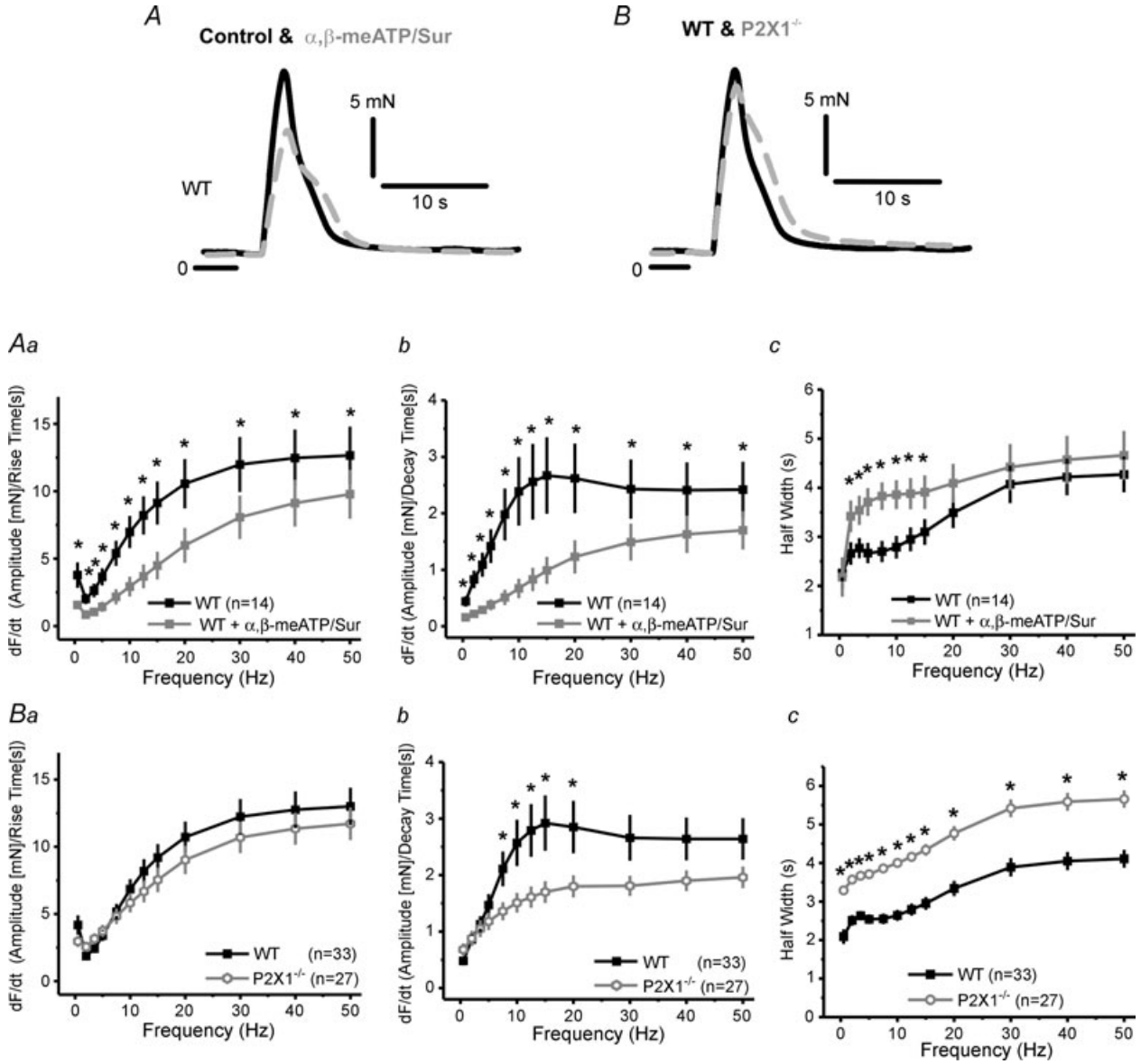

Figure 2. The kinetics of EFS-induced force transients from UBSM strips recorded from wild type (WT) and P2X1$^{-/-}$ urinary bladder smooth muscle strips

Single contractions in response to 10 Hz stimulation are recorded from (*A*) WT (control, continuous black line), and with purinergic block (α,β-meATP/suramin, 10 μM, dashed grey line) and, (*B*) WT (continuous black line) and P2X1$^{-/-}$ mice (dashed grey line). Rate of rise, rate of decay and half-width of the force transient are shown for WT (*Aa*, *Ab*, *Ac*) and for P2X1$^{-/-}$ (*Ba*, *Bb*, *Bc*) mice. $^*P < 0.05$.

Nerve stimulation evokes Ca^{2+} flashes

To study Ca^{2+} events in response to EFS, stimuli were applied at 10 Hz for 1 s and the temporal relationship between stimulation and the frequency of Ca^{2+} flashes was determined. To quantify Ca^{2+} flashes during stimulation, a stimulating frequency of 10 Hz was used. Higher stimulating frequencies would often evoke a sustained elevation in intracellular Ca^{2+}, making it difficult to accurately detect individual flashes during EFS. Figure 4 illustrates the nerve-evoked Ca^{2+} responses of different smooth muscle cells in the field of view. EFS induced an increase in Ca^{2+} flash activity. When EFS was stopped, Ca^{2+} flashes in a given cell either: (1) continued for a short period of time, (2) stopped altogether, or (3) redeveloped following a brief pause of 1–2 s. This second episode of Ca^{2+} flash activity continued for 6–8 s (Fig. 4*A* and *C*) in most cells but could last up to 16 s before decreasing to pre-EFS levels. The number of Ca^{2+} flashes following stimulation increased with an elevation of EFS frequency (Fig. 4*D–F*). The mean peak of Ca^{2+} flash activity after stimulation occurred about 5 s after EFS for each stimulating frequency (Fig. 4*D–F*). Ca^{2+} wave activity was difficult to measure during and after EFS in control, since the Ca^{2+} fluorescence is very intense during high-frequency firing of Ca^{2+} flashes. This made the detection of Ca^{2+} waves or other Ca^{2+} signals very difficult in fibres exhibiting Ca^{2+} flashes.

Inhibition of P2X1 receptors prevents Ca^{2+} flashes during EFS and increases Ca^{2+} flashes after stimulation

Inhibition of P2X1 receptors eliminated action potentials during EFS (Fig. 3*B* and *C*) and slowed the rate of rise of EFS-induced force (Fig. 2*A* and *Aa*). As expected from these results, inhibition of purinergic receptors with α,β-meATP–suramin prevented Ca^{2+} flashes during stimulation and exposed Ca^{2+} waves (Fig. 4*A–C*). In the examples shown in Fig. 4 (*Aa–d* and *Ba–d*), Ca^{2+} flash frequency increased and remained elevated after EFS up to 7 s before decreasing to pre-stimulus levels. However, following purinergic inhibition, in this case, Ca^{2+} flash

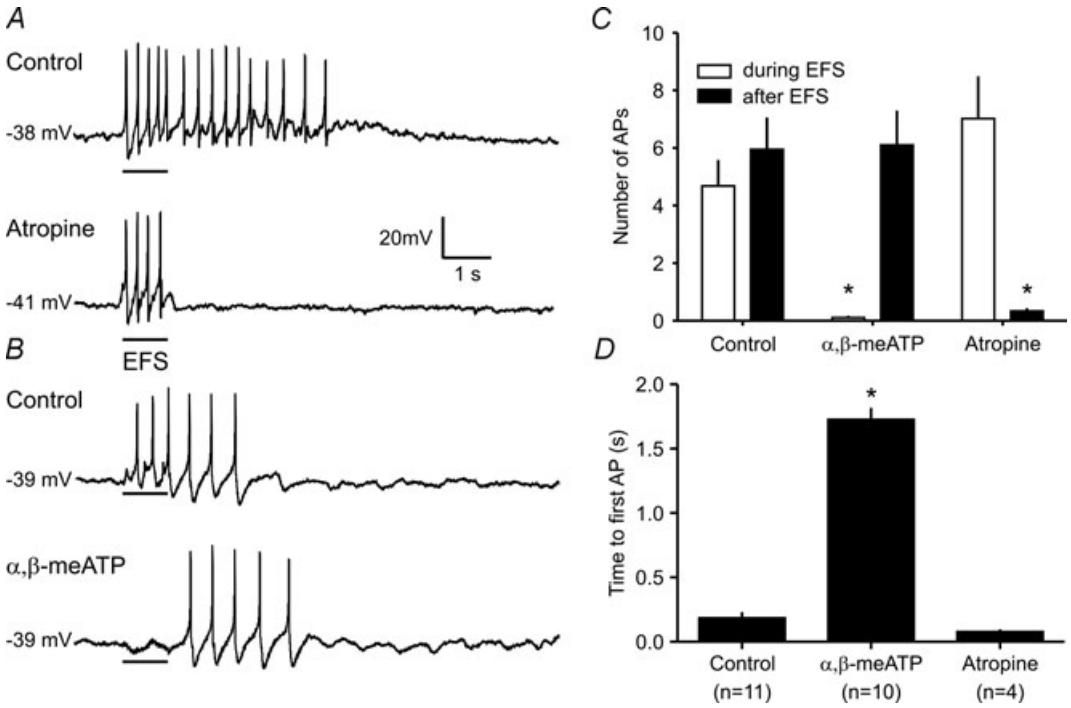

Figure 3. EFS induced purinergic-dependent action potentials during stimulation and muscarinic-dependent action potentials following stimulation
Intracellular recordings of membrane potential and action potentials from mouse detrusor evoked with 20 Hz (1 s) field stimulation. Action potentials are evoked with stimulation and continue after stimulation has stopped (*A* and *B*, upper traces). Inhibition of muscarinic receptors (atropine, 10 μM) (*A*, lower trace) does not affect the onset of action potentials during stimulation, but abolishes action potentials following stimulation. Inhibiting purinergic receptors (α,β-meATP, 10 μM) (*B*, lower trace) delays the onset of action potentials during stimulation. The number of action potentials (APs) is plotted during and after EFS for control and after purinergic and muscarinic receptor inhibition. The number of action potentials was significantly decreased during stimulation with purinergic block and after stimulation with muscarinic block (*C*). The time to the first action potential was significantly increased when purinergic receptors are inhibited (*D*). $^*P < 0.05$.

activity persisted for a longer period of time and was much more robust compared to control (Fig. 4*A*–*C*; see online Supplemental movies 1 and 2).

To compare Ca^{2+} flash activity in control and with muscarinic activation only (purinergic block), Ca^{2+} flash activity was plotted graphically during and up to 20 s after EFS (Fig. 5*A*). There were several striking differences in flash activity when P2X1 receptors were blocked. Ca^{2+} flash activity during EFS was very high in control, but nearly absent when P2X1 receptors were inactivated (Fig. 5*A*). In addition to eliminating flashes during stimulation, inhibition of purinergic receptors led

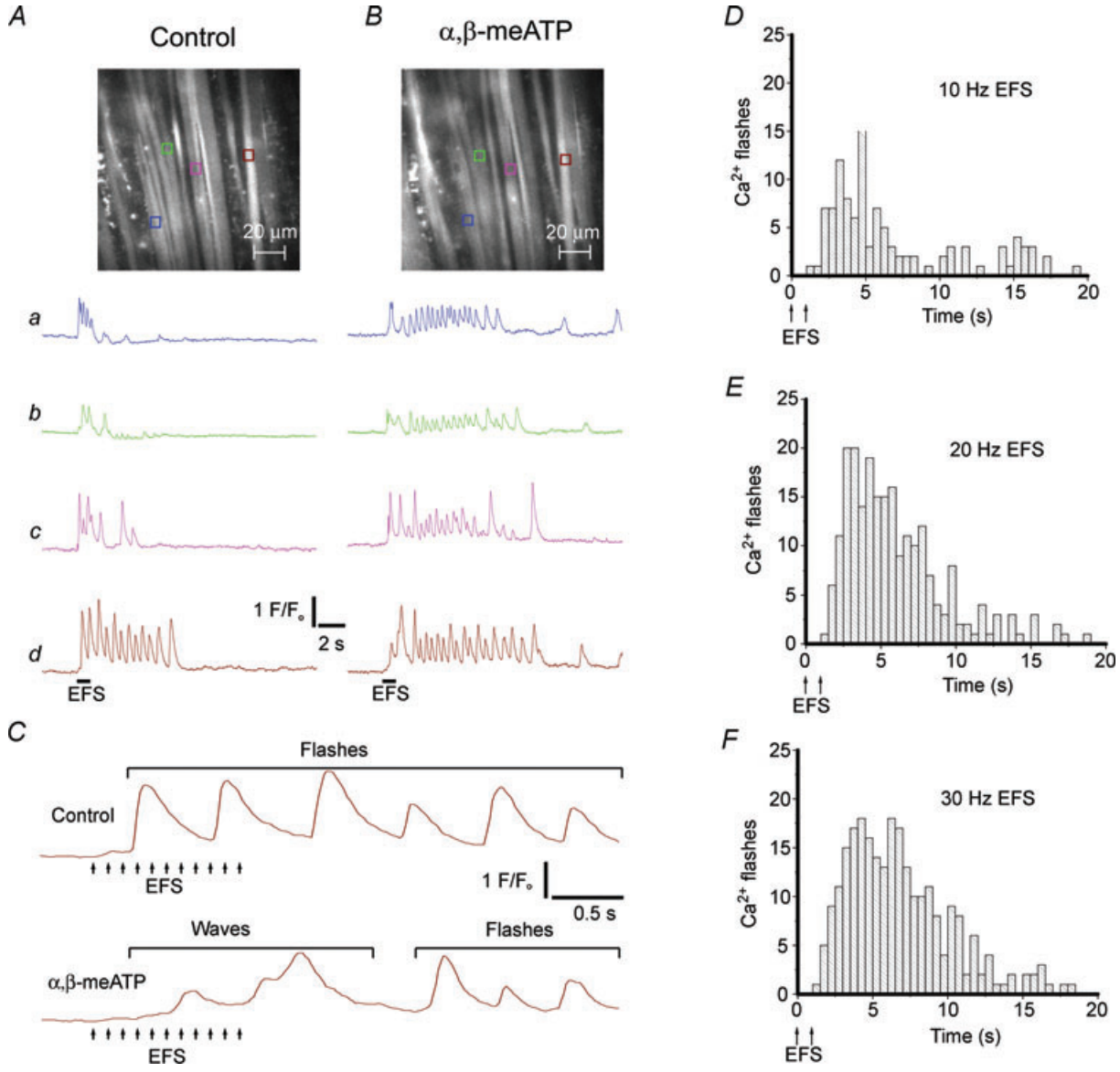

Figure 4. Ca^{2+} flashes in UBSM strips evoked with EFS (10 Hz) in control and after inhibition of P2X1 receptors with α,β-meATP (10 μM)

Images show vertically oriented grey smooth muscle bundles that increase in brightness when Ca^{2+} is elevated (*A* and *B*). Changes in Ca^{2+} in response to EFS in four regions of interest (ROI) (coloured boxes) in different cells before and after purinergic receptor inhibition are illustrated in *a*–*d* in *A* and *B*. Notice that the length of Ca^{2+} flash activity is increased after EFS when P2X1 receptors are inhibited (*Ba*–*d*). Ca^{2+} fluorescence from trace *d* is shown during and immediately after EFS at an expanded time frame (*C*). The Ca^{2+} flashes are evoked by EFS and continue after EFS in control (*C*, upper trace). With P2X1 inhibition, EFS evokes Ca^{2+} waves followed by Ca^{2+} flashes after EFS (*C*, lower trace) (see Supplemental movies 1 and 2). The number of Ca^{2+} flashes was measured following EFS (*D*–*F*). Ca^{2+} flashes during EFS were not measured since higher stimulating frequencies elevated intracellular Ca^{2+} during EFS making the detection of individual flashes difficult. The number of Ca^{2+} flashes following EFS were summed from 4 preparations and increased with stimulation frequency (10 Hz (*D*), 20 Hz (*E*) and 30 Hz (*F*)).

to a robust increase in the number of flashes (2-fold) and the length of elevated activity following stimulation (Fig. 5*A*). The response of Ca^{2+} flashes to EFS in P2X1$^{-/-}$ was the same as inactivating purinergic receptors in WT (Fig. 5). Ca^{2+} flashes were not evoked during EFS, but the number of flashes was greatly elevated following EFS when compared to WT (control) mice.

Muscarinic receptor block inhibits Ca^{2+} waves and Ca^{2+} flashes following stimulation

Inhibition of muscarinic receptors greatly reduced action potentials following EFS (Fig. 3*A* and *C*). Ca^{2+} flash activity following EFS was also greatly reduced by atropine at stimulation frequencies from 10 to 30 Hz (Fig. 6*A*–*C* and *E*). However, Ca^{2+} flash activity during EFS was unchanged (Fig. 6*D*), indicating that inhibition of muscarinic receptors did not alter purinergic-driven increases in excitability (see Supplemental movies 3 and 4). The block of Ca^{2+} flashes by atropine following EFS indicates that Ca^{2+} flashes (action potentials) are mediated through muscarinic activation. Atropine also significantly reduced Ca^{2+} waves. Using paired experiments (10 Hz EFS), atropine reduced Ca^{2+} waves by almost 90% (from 6.8 ± 2.3 waves cell^{-1} in control to 0.8 ± 0.8 waves cell^{-1}, $P < 0.05$, $n = 4$ strips). Inhibition of purinergic receptor function increased the number of EFS-induced Ca^{2+} waves (4.4 ± 2.7 waves field^{-1} in control to 12.4 ± 4.7 waves field^{-1} with purinergic block, $P < 0.05$, $n = 5$ strips). In the presence of purinergic inhibitors, EFS induced Ca^{2+} waves within 1 s, i.e. before the muscarinic-induced increases in Ca^{2+} flashes. These results are consistent with rapid engagement of muscarinic receptors by nerve-evoked release of ACh, an elevation of InsP_3 and Ca^{2+} waves during stimulation and a muscarinic-dependent delayed increase in excitability.

Discussion

Our results provide strong support for the concept that nerve-evoked release of ATP and ACh have different roles in shaping the contractile response of UBSM (Fig. 7). In response to a 1 s stimulation, ATP acts rapidly through P2X1R channels to increase UBSM excitability (action potentials) and Ca^{2+} entry (Ca^{2+} flashes), which is responsible for the rapid upstroke of force. The excitatory actions of ATP also terminate rapidly, on cessation of stimulation. Nerve-evoked release of ACh also has a profound excitatory effect, but its actions occur slowly and last longer (Fig. 7). Under the experimental conditions employed in this study, muscarinic-mediated increases in excitability started after stimulation and lasted 6–16 s. Loss of P2X1R functionality increased the muscarinic responses, as reflected in an elevation of frequency of Ca^{2+} flashes and an increase in duration of the force transient.

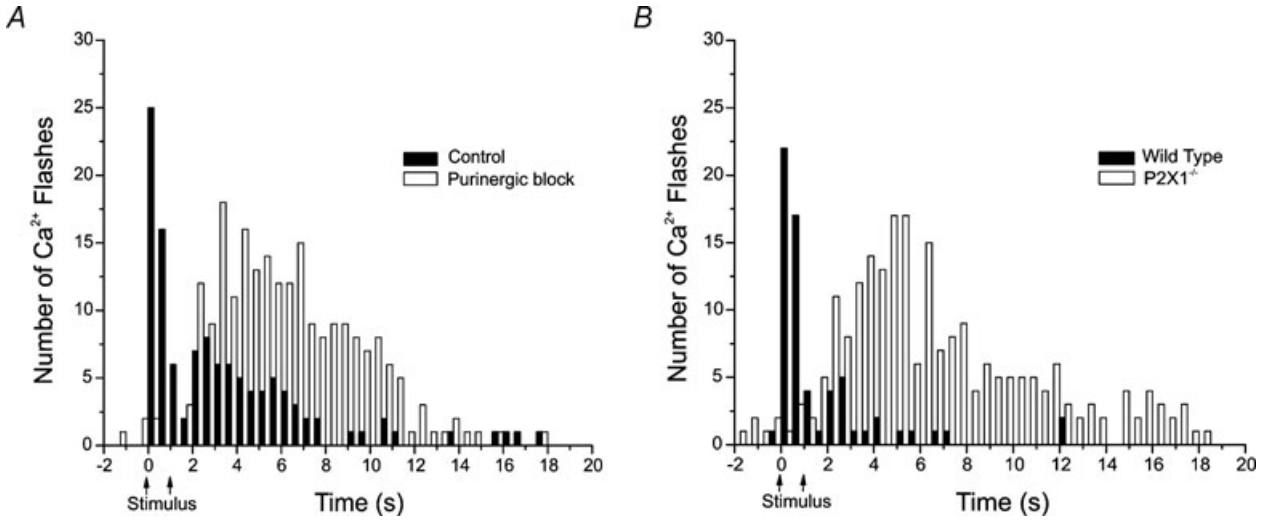

Figure 5. Loss of P2X1R function eliminates Ca^{2+} flashes during stimulation and increases post-stimulation Ca^{2+} flashes
Distribution of Ca^{2+} flashes during and following EFS (10 Hz, 1 s). Ca^{2+} flashes typically show two episodes of activity, one during EFS, and the second peaking between 2–8 s following EFS (*A*, control). Inhibition of purinergic receptors (α,β-meATP–suramin, 10 μM each) nearly abolishes Ca^{2+} flashes during EFS, but prolongs the second episode of Ca^{2+} flashes following EFS. Ca^{2+} flashes were obtained from paired experiments (4 preparations) in control and after inhibition of P2X1Rs (*A*). Similarly, when P2X1$^{-/-}$ were compared to WT, Ca^{2+} flashes during EFS were absent; however, the Ca^{2+} flashes following EFS were greatly increased (*B*). Ca^{2+} flashes were summed from 5 preparations (wild type) and 6 preparations (P2X1$^{-/-}$).

Mechanisms for the different time course of actions of nerve-evoked ATP and ACh

Nerve-evoked release of ATP acts rapidly to increase UBSM excitability because it activates an ion channel (P2X1Rs) to increase Na^+ and Ca^{2+} entry causing an excitatory junction potential (Hashitani *et al.* 2000; Young *et al.* 2008). Our results indicate that the purinergic effects dissipate rapidly upon cessation of stimulation, consistent with this mechanism. However, muscarinic-induced increase in excitability occurred after the cessation of stimulation (after 1 s, 10 Hz) and could last up to 16 s when purinergic signalling was inhibited. This response is consistent with ACh activating muscarinic (M_3) receptors and the engagement of slower second messenger pathways (InsP_3 and protein kinase C). We detected an atropine-sensitive increase in Ca^{2+} waves, with purinergic receptors inhibited, during the first second of stimulation, suggesting that InsP_3 has been elevated within this time frame (Fig. 4*C*). The mechanism by which muscarinic receptor stimulation increases UBSM excitability is not known. However, the muscarinic-driven increase in action potentials appears to be a major mechanism by which nerve stimulation increases contractility, and it appears to determine the duration of the force transient. In support of this, inhibitors of voltage-dependent Ca^{2+} channels, which are responsible for Ca^{2+} influx during an action potential, block nerve-evoked contractions of UBSM (Bo & Burnstock, 1990; Herrera *et al.* 2005).

In addition to the release of ATP and ACh, EFS may release peptides and other substances that modulate the force transient in UB (Andersson & Arner, 2004). For example, nitric oxide and calcitonin gene-related peptide

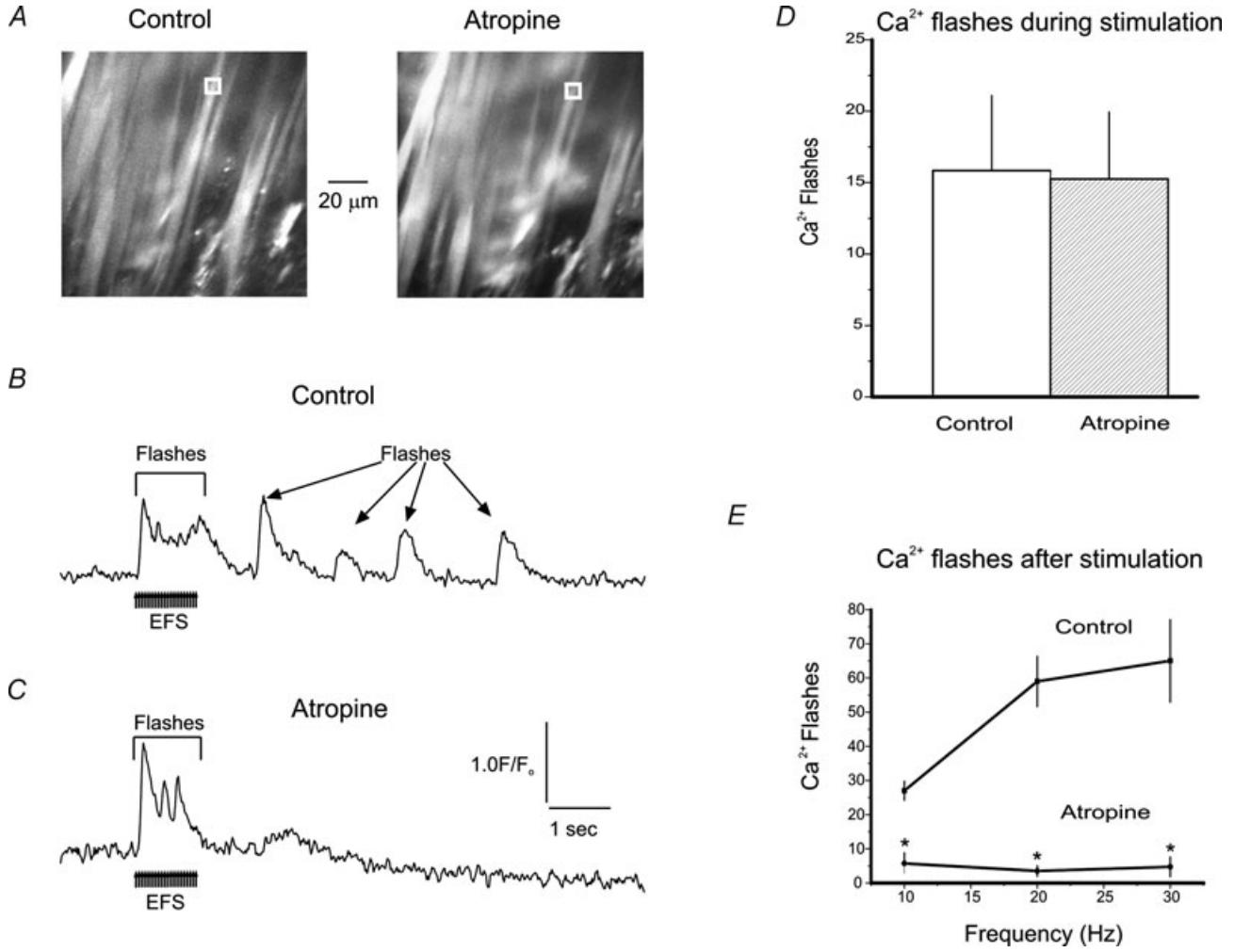

Figure 6. Activation of muscarinic receptors increases Ca^{2+} flashes
Ca^{2+} flashes recorded during EFS (20 Hz; 1 s) in control and after blocking the muscarinic pathway (atropine, 10 μM). Ca^{2+} fluorescence, recorded from the white box (*A*), shows Ca^{2+} flashes during and following EFS (20 Hz) (*B*). Inhibition of muscarinic receptors does not alter Ca^{2+} flashes during EFS (*C* and *D*), but greatly reduces flash activity following stimulation (*C* and *E*) (see Supplemental movies 3 and 4). Paired experiments from 4 preparations. $^*P < 0.05$.

are released from nerves and have a relaxing effect on UBSM (Andersson & Arner, 2004; Gillespie, 2005). A relaxing action on the force transient would be difficult to detect without specifically inhibiting the release of these factors. Compounds that elevate force would probably play a minor role since the elimination of purinergic and muscarinic pathways essentially abolished the contractions elicited by EFS (Fig. 1*Ac–Cc*).

P2X1 receptor-deficient mice have normal bladder function (Mulryan *et al.* 2000), and the muscarinic response to carbachol was not changed, suggesting that muscarinic receptor sensitivity and/or number are not altered (Vial & Evans, 2000). Ca^{2+} flash activity following stimulation is mediated through muscarinic receptors and is increased when purinergic signalling is absent (WT with purinergic receptors inhibited or $P2X1^{-/-}$ mice). Increased Ca^{2+} flash activity would elevate intracellular Ca^{2+} and force generation.

Possible mechanisms underlying purinergic inhibition of the muscarinic response

Loss of P2X1R function leads to an increase in Ca^{2+} flashes and duration of the force transient. The lack of a significant rise in action potentials, measured with microelectrodes, following purinergic receptor inhibition probably reflects the small number of action potentials that could be recorded from a single cell in a UBSM strip. In contrast, Ca^{2+} flashes could be recorded simultaneously from a larger number of cells. A number of possible mechanisms could potentially explain the inhibitory effect of P2X1Rs on muscarinic-induced increases in excitability.

In the present study, it is unlikely that the purinergic receptor inhibition of the muscarinic response is mediated pre-synaptically. P2X1 receptors in urinary bladder are located in postsynaptic smooth muscle membrane (Vial & Evans, 2000). The P2X1R inhibitory effects of P2X desensitizing agent (α,β-meATP) and antagonist (suramin) were the same as targeted disruption of the P2X1R gene (Figs 1, 2 and 5). Moreover, these drugs had no effect on UBSM strips from P2X1R-deficient mice (Fig. 1). These results suggest a postsynaptic mechanism through P2X1Rs.

ATP released from parasympathetic nerve varicosities rapidly activates P2X1R channels in UBSM membrane to cause Na^+ and Ca^{2+} influx, membrane potential depolarization and action potentials (Fig. 3) (Hashitani *et al.* 2000). The membrane potential depolarization and/or the increase in intracellular Ca^{2+} could conceivably have inhibitory effects on subsequent muscarinic-driven increases in excitability. L-type voltage-dependent Ca^{2+} channels are sensitive to membrane potential and Ca^{2+}, and can be inactivated by membrane depolarization and increasing concentrations of intracellular Ca^{2+} (Lacinova & Hofmann, 2005) as would occur during a burst of action potentials. The rapid membrane depolarization and onset

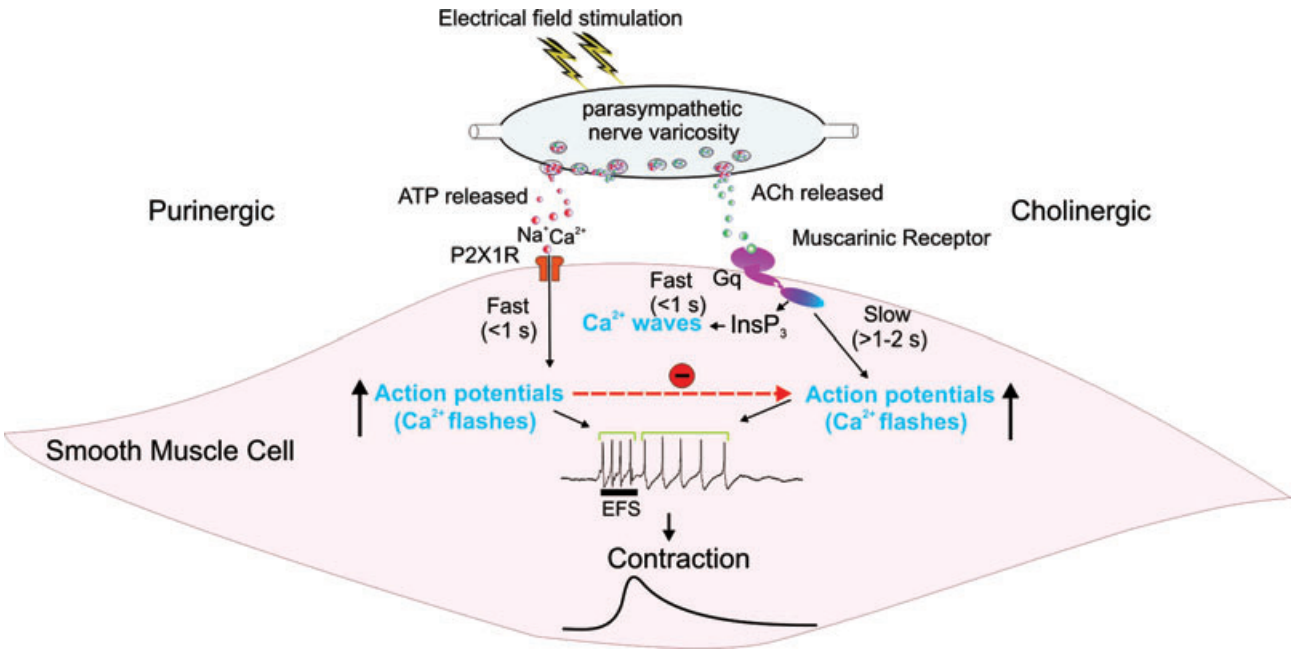

Figure 7. Schematic showing activation of purinergic and muscarinic pathways following release of neurotransmitters ATP and ACh from parasympathetic varicosities
Purinergic signalling rapidly evokes Ca^{2+} flashes during EFS whereas muscarinic signalling evokes Ca^{2+} waves during stimulation and Ca^{2+} flashes following stimulation. Purinergic activation appears to inhibit the muscarinic response. Ca^{2+} flashes from both purinergic and muscarinic pathways contribute to contraction.

of action potentials by purinergic receptor activation also activates voltage- and Ca^{2+}-sensitive K^+ channels (K_v, SK and BK channels), which could reduce subsequent membrane excitability (Fujii *et al.* 1990; Heppner *et al.* 1997; Hashitani & Brading, 2003*a*,*b*; Thorneloe & Nelson, 2003; Lacinova & Hofmann, 2005; Thorneloe *et al.* 2008). It is also possible that other Ca^{2+}-dependent processes may be involved in the suppression of muscarinic-mediated increases in excitability. These issues remain to be resolved by future studies.

Contribution of Ca^{2+} waves and Ca^{2+} flashes to force

Purinergic activation evokes Ca^{2+} flashes and muscarinic activation evokes both Ca^{2+} waves and Ca^{2+} flashes. Ca^{2+} flashes which reflect Ca^{2+} influx through L-type Ca^{2+} channels appear to be the major Ca^{2+} signal involved with contraction. Functional studies using mice deficient in the smooth muscle $Ca_v1.2$ Ca^{2+} channel (Wegener *et al.* 2004) as well as normal mouse bladder tissue (Herrera *et al.* 2005) indicate that L-type Ca^{2+} channels are critical for normal bladder function. We observed a muscarinic-driven increase in Ca^{2+} waves during stimulation and an increase in Ca^{2+} flashes following stimulation (Fig. 4*C*).

Evidence that Ca^{2+} waves play a minor role in generating force comes from studies using cyclopiazonic acid (CPA). CPA blocks Ca^{2+}-ATPase and prevents Ca^{2+} loading of the sarcoplasmic reticulum. If Ca^{2+} waves, which represent the release of Ca^{2+} from intracellular stores, contribute substantially to force we would expect force to be significantly decreased with CPA. However, in urinary bladder treated with CPA, force evoked by EFS was either unchanged (Munro & Wendt, 1994) or elevated (Ziganshin *et al.* 1994), suggesting that Ca^{2+} waves play a minor role in force generation.

Implications

ATP is co-released with ACh from parasympathetic nerves as well as with noradrenaline (norepinephrine) from sympathetic nerves (Burnstock, 1986, 1990, 2009; Westfall *et al.* 2002). ATP acts on P2X1Rs to cause rapid excitation. Our results indicate that P2X1R effects could modulate both muscarinic and adrenergic effects on the post-synaptic cell. This influence is inhibitory for urinary bladder smooth muscle (this study), but it could also have a potentiating effect, as well, depending on the nature of the cell and mechanisms engaged. Our results also have a general implication for interpretation of the purinergic mechanisms to nerve-evoked force generation: A reduction of peak contraction by purinergic receptor inhibition can not be used to determine purinergic contributions, if P2X1R activation modulates subsequent muscarinic/adrenergic responses.

The interaction between excitatory pathways may be significant in light of the elevated purinergic and diminished muscarinic contributions in certain human bladder pathologies. In contrast to rodents, where muscarinic and purinergic pathways significantly contribute to force generation (Andersson & Arner, 2004), nearly 100% of bladder contraction in normal human bladder is due to muscarinic activation (Hindmarsh *et al.* 1977; Sibley, 1984; Bayliss *et al.* 1999). However, with some bladder pathologies, such as cystitis or overactive bladder, the atropine-resistant, purinergic component in human bladder increases dramatically and reaches 30–50% (Palea *et al.* 1993; Bayliss *et al.* 1999; O'Reilly *et al.* 2001). Two common urological problems are overactive bladder, a condition where the detrusor contracts involuntarily during filling, and detrusor underactivity, a condition where bladder contractility is diminished. There is evidence that overactive bladder may be due to an augmentation of purinergic signalling (Palea *et al.* 1993; Andersson, 2003; Yoshida *et al.* 2004) while detrusor underactivity probably results from reduced force generated by the muscarinic pathway (Taylor & Kuchel, 2006). Detrusor hyperactivity with impaired contractile function (DHIC) is a combination of detrusor overactivity and detrusor underactivity (Resnick & Yalla, 1987). It is a common urodynamic finding and may occur in up to one third of incontinent nursing home residents (Resnick *et al.* 1989; Taylor & Kuchel, 2006). Management of DHIC is difficult since antispasmodic anticholinergic medications that are commonly used to treat overactive bladder may worsen retention, whereas no effective pharmacotherapy exists for detrusor underactivity (Taylor & Kuchel, 2006). The findings from the present study show that purinergic activation inhibits the muscarinic response in mouse urinary bladder. If a similar purinergic–muscarinic interaction occurs in human bladder, this mechanism could underlie or contribute to DHIC. If indeed the elevated purinergic component in human bladder pathologies was contributing to involuntary detrusor contractions as well as suppressing muscarinic force, inhibition of the purinergic response would not only decrease symptoms of purinergic-mediated overactive bladder, but also relieve the purinergic-mediated inhibition of muscarinic contraction. The development of therapeutics to target the purinergic response may hold promise to alleviate clinical symptoms of DHIC.

Conclusions

Nerve-evoked release of ATP and ACh leads to a rapid increase in excitability due to P2X1R activation and a slower and longer increase in excitability due

to muscarinic receptor activation. As a consequence, P2X1Rs mediate the rapid rise in force and muscarinic receptor activation determines the duration of the force transient. In addition, P2X1R contributions to force generation are more significant at lower stimulation frequencies. We have also identified a novel, post-synaptic, modulatory mechanism by which P2X1R activation suppresses subsequent muscarinic-mediated increases in excitability and force generation. These results suggest the potential for postsynaptic modulation of excitability in other P2X-containing tissues because ATP is co-released with other Gq-coupled neurotransmitters (e.g. noradrenaline). Postjunctional modulation of neurotransmitter actions could alter target tissue responses, and may be involved in a number of clinical conditions (e.g. DHIC, cystitis, outlet obstruction, overactive bladder and detrusor underactivity).

References

Abrams P & Andersson KE (2007). Muscarinic receptor antagonists for overactive bladder. *BJU Int* **100**, 987–1006.

Andersson KE (2003). Storage and voiding symptoms: pathophysiologic aspects. *Urology* **62**, 3–10.

Andersson KE & Arner A (2004). Urinary bladder contraction and relaxation: physiology and pathophysiology. *Physiol Rev* **84**, 935–986.

Balemba OB, Salter MJ, Heppner TJ, Bonev AD, Nelson MT & Mawe GM (2006). Spontaneous electrical rhythmicity and the role of the sarcoplasmic reticulum in the excitability of guinea pig gallbladder smooth muscle cells. *Am J Physiol Gastrointest Liver Physiol* **290**, G655–G664.

Bayliss M, Wu C, Newgreen D, Mundy AR & Fry CH (1999). A quantitative study of atropine-resistant contractile responses in human detrusor smooth muscle, from stable, unstable and obstructed bladders. *J Urol* **162**, 1833–1839.

Bo XN & Burnstock G (1990). The effects of Bay K 8644 and nifedipine on the responses of rat urinary bladder to electrical field stimulation, β,γ-methylene ATP and acetylcholine. *Br J Pharmacol* **101**, 494–498.

Brain KL, Cuprian AM, Williams DJ & Cunnane TC (2003). The sources and sequestration of Ca^{2+} contributing to neuroeffector Ca^{2+} transients in the mouse vas deferens. *J Physiol* **553**, 627–635.

Brain KL, Jackson VM, Trout SJ & Cunnane TC (2002). Intermittent ATP release from nerve terminals elicits focal smooth muscle Ca^{2+} transients in mouse vas deferens. *J Physiol* **541**, 849–862.

Burnstock G (1986). Purines and cotransmitters in adrenergic and cholinergic neurones. *Prog Brain Res* **68**, 193–203.

Burnstock G (1990). Local mechanisms of blood flow control by perivascular nerves and endothelium. *J Hypertens Suppl* **8**, S95–S106.

Burnstock G (2009). Purinergic cotransmission. *Exp Physiol* **94**, 20–24.

Drummond GB (2009). Reporting ethical matters in *The Journal of Physiology*: standards and advice. *J Physiol* **587**, 713–719.

Fetscher C, Fleichman M, Schmidt M, Krege S & Michel MC (2002). M_3 muscarinic receptors mediate contraction of human urinary bladder. *Br J Pharmacol* **136**, 641–643.

Fujii K, Foster CD, Brading AF & Parekh AB (1990). Potassium channel blockers and the effects of cromakalim on the smooth muscle of the guinea-pig bladder. *Br J Pharmacol* **99**, 779–785.

Gillespie JI (2005). Inhibitory actions of calcitonin gene-related peptide and capsaicin: evidence for local axonal reflexes in the bladder wall. *BJU Int* **95**, 149–156.

Gitterman DP & Evans RJ (2001). Nerve evoked P2X receptor contractions of rat mesenteric arteries; dependence on vessel size and lack of role of L-type calcium channels and calcium induced calcium release. *Br J Pharmacol* **132**, 1201–1208.

Hashitani H & Brading AF (2003*a*). Electrical properties of detrusor smooth muscles from the pig and human urinary bladder. *Br J Pharmacol* **140**, 146–158.

Hashitani H & Brading AF (2003*b*). Ionic basis for the regulation of spontaneous excitation in detrusor smooth muscle cells of the guinea-pig urinary bladder. *Br J Pharmacol* **140**, 159–169.

Hashitani H, Bramich NJ & Hirst GD (2000). Mechanisms of excitatory neuromuscular transmission in the guinea-pig urinary bladder. *J Physiol* **524**, 565–579.

Heppner TJ, Bonev AD & Nelson MT (1997). Ca^{2+}-activated K^+ channels regulate action potential repolarization in urinary bladder smooth muscle. *Am J Physiol Cell Physiol* **273**, C110–C117.

Heppner TJ, Bonev AD & Nelson MT (2005). Elementary purinergic Ca^{2+} transients evoked by nerve stimulation in rat urinary bladder smooth muscle. *J Physiol* **564**, 201–212.

Herrera GM, Etherton B, Nausch B & Nelson MT (2005). Negative feedback regulation of nerve-mediated contractions by KCa channels in mouse urinary bladder smooth muscle. *Am J Physiol Regul Integr Comp Physiol* **289**, R402–R409.

Hindmarsh JR, Idowu OA, Yeates WK & Zar MA (1977). Pharmacology of electrically evoked contractions of human bladder [proceedings]. *Br J Pharmacol* **61**, 115P.

Iacovou JW, Hill SJ & Birmingham AT (1990). Agonist-induced contraction and accumulation of inositol phosphates in the guinea-pig detrusor: evidence that muscarinic and purinergic receptors raise intracellular calcium by different mechanisms. *J Urol* **144**, 775–779.

Iino M (1990). Biphasic Ca^{2+} dependence of inositol 1,4,5-trisphosphate-induced Ca release in smooth muscle cells of the guinea pig taenia caeci. *J Gen Physiol* **95**, 1103–1122.

Iino M, Yamazawa T, Miyashita Y, Endo M & Kasai H (1993). Critical intracellular Ca^{2+} concentration for all-or-none Ca^{2+} spiking in single smooth muscle cells. *EMBO J* **12**, 5287–5291.

Ji G, Feldman ME, Deng KY, Greene KS, Wilson J, Lee JC, Johnston RC, Rishniw M, Tallini Y, Zhang J, Wier WG, Blaustein MP, Xin HB, Nakai J & Kotlikoff MI (2004). Ca^{2+}-sensing transgenic mice: postsynaptic signalling in smooth muscle. *J Biol Chem* **279**, 21461–21468.

Klockner U & Isenberg G (1985). Calcium currents of cesium loaded isolated smooth muscle cells (urinary bladder of the guinea pig). *Pflugers Arch* **405**, 340–348.

Lacinova L & Hofmann F (2005). Ca^{2+}- and voltage-dependent inactivation of the expressed L-type $Ca_v1.2$ calcium channel. *Arch Biochem Biophys* **437**, 42–50.

Lamont C, Vainorius E & Wier WG (2003). Purinergic and adrenergic Ca^{2+} transients during neurogenic contractions of rat mesenteric small arteries. *J Physiol* **549**, 801–808.

Lamont C & Wier WG (2002). Evoked and spontaneous purinergic junctional Ca^{2+} transients (jCaTs) in rat small arteries. *Circ Res* **91**, 454–456.

McCarron JG, MacMillan D, Bradley KN, Chalmers S & Muir TC (2004). Origin and mechanisms of Ca^{2+} waves in smooth muscle as revealed by localized photolysis of caged inositol 1,4,5-trisphosphate. *J Biol Chem* **279**, 8417–8427.

Matsui M, Motomura D, Karasawa H, Fujikawa T, Jiang J, Komiya Y, Takahashi S & Taketo MM (2000). Multiple functional defects in peripheral autonomic organs in mice lacking muscarinic acetylcholine receptor gene for the M3 subtype. *Proc Natl Acad Sci U S A* **97**, 9579–9584.

Mulryan K, Gitterman DP, Lewis CJ, Vial C, Leckie BJ, Cobb AL, Brown JE, Conley EC, Buell G, Pritchard CA & Evans RJ (2000). Reduced vas deferens contraction and male infertility in mice lacking P2X1 receptors. *Nature* **403**, 86–89.

Munro DD & Wendt IR (1994). Effects of cyclopiazonic acid on $[Ca^{2+}]_i$ and contraction in rat urinary bladder smooth muscle. *Cell Calcium* **15**, 369–380.

O'Reilly BA, Kosaka AH, Chang TK, Ford AP, Popert R, Rymer JM & McMahon SB (2001). A quantitative analysis of purinoceptor expression in human fetal and adult bladders. *J Urol* **165**, 1730–1734.

Palea S, Artibani W, Ostardo E, Trist DG & Pietra C (1993). Evidence for purinergic neurotransmission in human urinary bladder affected by interstitial cystitis. *J Urol* **150**, 2007–2012.

Resnick NM & Yalla SV (1987). Detrusor hyperactivity with impaired contractile function. An unrecognized but common cause of incontinence in elderly patients. *JAMA* **257**, 3076–3081.

Resnick NM, Yalla SV & Laurino E (1989). The pathophysiology of urinary incontinence among institutionalized elderly persons. *N Engl J Med* **320**, 1–7.

Sibley GN (1984). A comparison of spontaneous and nerve-mediated activity in bladder muscle from man, pig and rabbit. *J Physiol* **354**, 431–443.

Takeuchi T, Yamashiro N, Kawasaki T, Nakajima H, Azuma YT & Matsui M (2008). The role of muscarinic receptor subtypes in acetylcholine release from urinary bladder obtained from muscarinic receptor knockout mouse. *Neuroscience* **156**, 381–389.

Taylor JA 3rd & Kuchel GA (2006). Detrusor underactivity: Clinical features and pathogenesis of an underdiagnosed geriatric condition. *J Am Geriatr Soc* **54**, 1920–1932.

Thorneloe KS, Knorn AM, Doetsch PE, Lashinger ES, Liu AX, Bond CT, Adelman JP & Nelson MT (2008). Small-conductance, Ca^{2+}-activated K^+ channel 2 is the key functional component of SK channels in mouse urinary bladder. *Am J Physiol Regul Integr Comp Physiol* **294**, R1737–R1743.

Thorneloe KS & Nelson MT (2003). Properties and molecular basis of the mouse urinary bladder voltage-gated K^+ current. *J Physiol* **549**, 65–74.

Vial C & Evans RJ (2000). P2X receptor expression in mouse urinary bladder and the requirement of $P2X_1$ receptors for functional P2X receptor responses in the mouse urinary bladder smooth muscle. *Br J Pharmacol* **131**, 1489–1495.

Wegener JW, Schulla V, Lee TS, Koller A, Feil S, Feil R, Kleppisch T, Klugbauer N, Moosmang S, Welling A & Hofmann F (2004). An essential role of Cav1.2 L-type calcium channel for urinary bladder function. *FASEB J* **18**, 1159–1161.

Werner ME, Knorn AM, Meredith AL, Aldrich RW & Nelson MT (2007). Frequency encoding of cholinergic- and purinergic-mediated signalling to mouse urinary bladder smooth muscle: modulation by BK channels. *Am J Physiol Regul Integr Comp Physiol* **292**, R616–R624.

Westfall DP, Todorov LD & Mihaylova-Todorova ST (2002). ATP as a cotransmitter in sympathetic nerves and its inactivation by releasable enzymes. *J Pharmacol Exp Ther* **303**, 439–444.

Yamanishi T, Chapple CR, Yasuda K & Chess-Williams R (2000). The role of M_2-muscarinic receptors in mediating contraction of the pig urinary bladder *in vitro*. *Br J Pharmacol* **131**, 1482–1488.

Yoshida M, Miyamae K, Iwashita H, Otani M & Inadome A (2004). Management of detrusor dysfunction in the elderly: changes in acetylcholine and adenosine triphosphate release during aging. *Urology* **63**, 17–23.

Young JS, Meng E, Cunnane TC & Brain KL (2008). Spontaneous purinergic neurotransmission in the mouse urinary bladder. *J Physiol* **586**, 5743–5755.

Ziganshin AU, Hoyle CH, Ziganshina LE & Burnstock G (1994). Effects of cyclopiazonic acid on contractility and ecto-ATPase activity in guinea-pig urinary bladder and vas deferens. *Br J Pharmacol* **113**, 669–674.

Acknowledgements

This work was supported in part by the Totman Trust and NIH grants DK053832 and DK065947 to M.T.N., the British Heart Foundation (PG/07/115) to M.E.W., and the Wellcome Trust to R.J.E.. We wish to thank Anna-Maria Knorn for her technical assistance on the myography studies.